Spin-polarized STM for a Kondo adatom

2009 J. Phys.: Condens. Matter 21 095003

(http://iopscience.iop.org/0953-8984/21/9/095003)

J. Phys.: Condens. Matter **21** (2009) 095003 (7pp) doi:10.1088/0953-8984/21/9/095003

Spin-polarized STM for a Kondo adatom

A C Seridonio[1,2], F M Souza[1] and I A Shelykh[1,3]

[1] ICCMP-International Center for Condensed Matter Physics, Universidade de Brasília, 04513 Brasília, DF, Brazil
[2] Instituto de Física, Universidade Federal Fluminense, 24310-246, Niterói, RJ, Brazil
[3] Science Department, University of Iceland, Dunhaga 3, IS-107, Reykjavik, Iceland

E-mail: fmsouza@unb.br

Received 13 October 2008, in final form 8 December 2008
Published 29 January 2009
Online at stacks.iop.org/JPhysCM/21/095003

Abstract
We investigate the bias dependence of the tunneling conductance between a spin-polarized (SP) scanning tunneling microscope (STM) tip and the surface conduction states of a normal metal with a Kondo adatom. Quantum interference between tip–host metal and tip–adatom–host metal conduction paths is studied in the full range of the Fano parameter q. The spin-polarized STM gives rise to a splitting of the Kondo peak and asymmetry in the zero-bias anomaly, depending on the lateral tip–adatom distance. For increasing lateral distances, the Kondo peak splitting shows a strong suppression and the spin-polarized conductance exhibits the standard Fano–Kondo profile.

(Some figures in this article are in colour only in the electronic version)

1. Introduction

The Kondo effect is an antiferromagnetic screening of a localized magnetic moment by the host metallic electrons below a characteristic Kondo temperature T_K, which results in the appearance of an additional peak in the system's density of states pinned to the Fermi energy. Being first observed during studies of transport properties of bulk diluted magnetic alloys [1], the Kondo effect was later on shown to affect the conductance of single quantum dots (QDs) [2, 3], arrays of QDs [4, 5] and possibly quantum point contacts [6, 7]. In the emerging field of spintronics [8], the coupling of a single QD to ferromagnetic leads can shed more light on fundamental aspects of the Kondo physics and provide a basis for a design of novel spintronic components [9–17].

The scanning tunneling microscope (STM) is widely used for investigation of the Kondo effect at surfaces of normal metals with adsorbed magnetic impurities (Kondo adatoms) [18–26]. The possible examples are individual Co atoms at Au(111), Cu(100) or Cu(111) surfaces [18–21], and cobalt carbonyl $Co(CO)_n$ complexes or manganese phthalocyanine (MnPc) molecules on top of Pb islands [22, 23].

In the present work we focus on the Kondo regime for a system containing a ferromagnetic STM tip and a single Kondo adatom on a metallic surface (figure 1). In this system the conductance becomes spin-dependent, due to the ferromagnetic (FM) tip, which leads to a Zeeman splitting in the Kondo adatom density of states (DOS). Particular attention is paid to the interplay between Kondo effect, quantum interference of two possible tunneling paths (tip–adatom–host and tip–host) and the ferromagnetism of the tip.

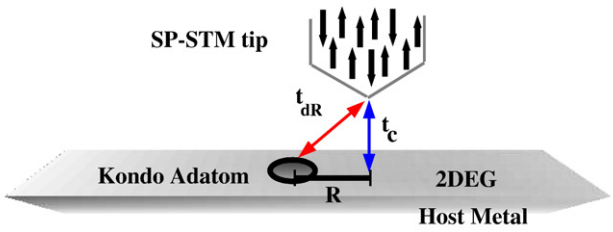

Figure 1. Set-up of the SP-STM and the host metal with the Kondo adatom. The interference between the channels t_{dR} and t_c exhibits a spin-polarized Fano–Kondo profile for the conductance.

Our study differs from previous work in the same field [27] mainly in the three aspects described below.

First. We present new results for the tunneling conductance as a function of the bias for different lateral tip–adatom separations R in the Kondo regime. This is an actual task indeed, as in experiments with unpolarized systems, R was shown to strongly affect the conductance [18, 19]. For ferromagnetic tips, however, corresponding results are lacking.

Second. We discuss the small, large and intermediate cases for the Fano parameter[4] q [28–31]. We show that

[4] The Fano parameter q gives the strength of the quantum interference between different tunneling paths. It is proportional to the ratio between the tip–adatom and tip–host hopping coefficients.

the three cases above give different conductance patterns. Experimentally, the large and small q limits are relevant and have been realized for unpolarized conduction bands. For example, in [21] it was shown that q alternates from intermediate ($q \approx 1.13$) to small ($q \approx 0.18$) values by changing the Cu crystal surface (Cu(100) and Cu(111)), in which a Co adatom is deposited. The conductance profile for the small q limit can also be experimentally observed in quantum corrals [19]. Alternatively, manipulating the molecular structure of the magnetic impurity on the Cu(100) surface, it is possible to switch between the intermediate and large q limits [22, 23].

Third. Instead of using a Lorentzian approximation for the Kondo peak, we apply the well-established Doniach–Sunjic formula [32, 33], whose validity is supported by numerical calculations based on both numerical renormalization group [32, 33], quantum Monte Carlo simulations [34] and by the recent success in fitting experimental data [23].

Our results show that, for a tip situated right above the Kondo adatom ($R = 0$), asymmetric zero-bias anomalies appear, which are revealed as resonances and anti-resonances in the conductance in the limits of large and small q, respectively. For $q \approx 1$, the conductance demonstrates a pronounced plateau in the region of small biases ($eV \approx 0$). The increase of R leads to a suppression of the tip-induced adatom's Zeeman splitting, thus resulting in a conductance pattern that resembles experimental data for unpolarized systems [18]. Finally, we verify that the Kondo peak splitting strongly depends on the asymmetry between the tip–adatom and adatom–host tunnelings.

This paper is organized as follows. In section 1 we present the model adopted to describe the system under study. In section 2 we derive an expression for the spin-resolved conductance based on a perturbative expansion for the tunneling Hamiltonian. In section 3 we discuss the numerical results. Conclusions are presented in section 4.

2. The model

The description of the metallic host and its interaction with the adatom is performed within the framework of the single impurity Anderson model [35] with a half-filled noninteracting conduction band:

$$H_{\rm A} = \sum_{\sigma} \int \varepsilon c^{\dagger}_{\varepsilon\sigma} c_{\varepsilon\sigma}\, {\rm d}\varepsilon + \sum_{\sigma} \varepsilon_{d\sigma} d^{\dagger}_{\sigma} d_{\sigma} + U n_{d\uparrow} n_{d\downarrow} + \sqrt{\frac{\Gamma}{\pi}} \sum_{\sigma} \int {\rm d}\varepsilon (c^{\dagger}_{\varepsilon\sigma} d_{\sigma} + {\rm H.c.}), \quad (1)$$

where all energies are measured from the Fermi level coinciding with the center of the band ($\varepsilon_{\rm F} = 0$) and extend from $-D$ to D. The operator

$$c_{\varepsilon\sigma} = \rho_0^{-1/2} \sum_{\vec{k}} c_{\vec{k}\sigma} \delta(\varepsilon - \varepsilon_k), \quad (2)$$

corresponds to a surface conduction state of the host metal with an energy-independent density of states per spin ρ_0.

The first term in equation (1) describes a two-dimensional electron gas (2DEG) on the surface of a host metal. The second and the third correspond to the adatom, which is characterized by a single-particle orbital energy $\varepsilon_{d\sigma}$ and Coulomb repulsion U. The last term, proportional to $\sqrt{\Gamma}$, describes the coupling between the adatom and the host metal conduction states, thus introducing the broadenings of the adatom's resonances at the energies $\varepsilon_{d\sigma}$ and $\varepsilon_{d\sigma} + U$. In the Kondo regime ($T \ll T_{\rm K}, \varepsilon_{d\sigma} < \varepsilon_{\rm F}, \varepsilon_{d\sigma} + U > \varepsilon_{\rm F}$, $\Gamma \ll |\varepsilon_{d\sigma}|$, $\varepsilon_{d\sigma} + U$) an additional peak in the density of states having a half-width $\Gamma_{\rm K} = k_{\rm B} T_{\rm K}$ ($k_{\rm B}$ is the Boltzmann constant and $T_{\rm K}$ is the Kondo temperature)[5] appears exactly at the Fermi level.

The total STM Hamiltonian is

$$H_{\rm STM} = H_{\rm A} + H_{\rm tip} + H_{\rm tun}, \quad (3)$$

where $H_{\rm tip}$ corresponds to free electrons in the tip:

$$H_{\rm tip} = \sum_{\vec{p}\sigma} (\varepsilon_{\vec{p}} + eV) a^{\dagger}_{\vec{p}\sigma} a_{\vec{p}\sigma}, \quad (4)$$

with the operators $a_{\vec{p}\sigma}$ describing the bulk conduction states, the bias is eV and

$$H_{\rm tun} = \sum_{\vec{p}\sigma} [t^{\sigma}_{\rm c} a^{\dagger}_{\vec{p}\sigma} B_{\sigma}(\vec{R}) + {\rm H.c.}] \quad (5)$$

is the tunneling Hamiltonian that connects the tip with the host metal via the operator

$$B_{\sigma}(\vec{R}) = \left[\int \tilde{N}_{\varepsilon}^{-1} \tilde{C}_{\varepsilon\sigma}\, {\rm d}\varepsilon + q^{\sigma}_{R} \sqrt{\pi\Gamma\rho_0} d_{\sigma} \right]. \quad (6)$$

The normalization factor in equation (6) is

$$\tilde{N}_{\varepsilon} = \left[\sum_{\vec{k}} |\varphi_{\vec{k}}(\vec{R})|^2 \delta(\varepsilon - \varepsilon_k) \right]^{-1/2}, \quad (7)$$

with $\varphi_{\vec{k}}(\vec{R}) \sim {\rm e}^{{\rm i}\vec{k}\vec{R}}$ being a wavefunction of the host conduction electron.

The first term in equation (6) containing the operator

$$\tilde{C}_{\varepsilon\sigma} = \tilde{N}_{\varepsilon} \sum_{\vec{k}} \varphi_{\vec{k}}(\vec{R}) c_{\vec{k}\sigma} \delta(\varepsilon - \epsilon_k), \quad (8)$$

hybridizes the conduction states of the tip with the surface of the host at a displaced lateral position $\vec{R}$ from the adatom.

The second term describes the tunneling between the tip and localized adatom's level characterized by a spin-dependent parameter (Fano factor) [37, 38]

$$q^{\sigma}_{R} = (\pi\Gamma\rho_0)^{-1/2} (t^{\sigma}_{dR}/t^{\sigma}_{\rm c}), \quad (9)$$

defined as a ratio between the couplings t^{σ}_{dR} of the tip–adatom and $t^{\sigma}_{\rm c}$ of the tip–host metal.

The Fano factor monitors the competition between the tunneling channels in the system. It vanishes with the increase of the tip–adatom lateral distance R, which can be modeled by an exponentially decaying function [38]

$$q^{\sigma}_{R} = q^{\sigma}_{R=0} {\rm e}^{-k_{\rm F} R}. \quad (10)$$

[5] The Kondo temperature is calculated according to equation (24) of [36] $k_{\rm B} T_{\rm K} = \sqrt{\Gamma U/2} \exp[\pi \varepsilon^0_d (\varepsilon^0_d + U)/2\Gamma U]$, where ε^0_d is the energy of the adatom's occupied level.

The decay of the Fano parameter with the increasing of the lateral tip–adatom distance was already experimentally explored in a system with a Co adatom on a Cu surface [21]. Indeed, the precise value of the Fano factor should be determined from first-principles calculations of the hopping elements t_c^σ and t_{dR}^σ, which depend on the choice of the STM tip, host surface and adatom. As the interest here is to analyze the conductance lineshape for the entire range of the Fano factor, we consider it as a free parameter of the model, with small, intermediate and large adopted values in the simulations (see section 4).

In the present work we consider a ferromagnetic tip with a spin-dependent density of states given by

$$\rho_{\rm tip}^\sigma = \rho_0[1 + \sigma P_{\rm tip}], \tag{11}$$

where $\sigma = +$ or $-$ for spins $\uparrow$ or $\downarrow$, respectively, and $P_{\rm tip}$ is a polarization degree of the tip. The inequality between spin-up and spin-down populations in the tip $\rho_{\rm tip}^{\uparrow} > \rho_{\rm tip}^{\downarrow}$ introduces an asymmetry in the splitting of the zero-bias anomaly as we will see in section 4. The density of states for the unpolarized tip $\rho_0 = \rho_{\rm tip}(\varepsilon_{\rm F})$ is assumed to be equal to the density of states of the host metal for simplicity.

3. Methodology

We calculate the tunneling conductance of the system treating the coupling between tip and host metal ($H_{\rm tun}$) as a perturbation. Within a second-order perturbation scheme, the formula for the conductance [37] is

$$G = (e^2/h)\sum_\sigma \int T_\sigma(\varepsilon, T, R, q_R^\sigma)\left[-\frac{\partial}{\partial\varepsilon} f(\varepsilon - eV)\right] {\rm d}\varepsilon, \tag{12}$$

where

$$T_\sigma(\varepsilon, T, R, q_R^\sigma) = T_{o\sigma}\{1 + |q_R^\sigma|^2\}(\rho_{\rm tip}^\sigma/\rho_0)(\rho_{\rm LDOS}^\sigma/\rho_0), \tag{13}$$

is an effective transmission coefficient with

$$T_{o\sigma} = (2\pi\rho_0 t_c^\sigma)^2. \tag{14}$$

The local density of states (LDOS) appearing in equation (13) is defined as

$$\rho_{\rm LDOS}^\sigma = -\frac{1}{\pi}\frac{{\rm Im}\langle\langle B_\sigma(\vec{R})|B_\sigma^\dagger(\vec{R})\rangle\rangle_\varepsilon}{1 + |q_R^\sigma|^2}, \tag{15}$$

with $\langle\langle B_\sigma(\vec{R})|B_\sigma^\dagger(\vec{R})\rangle\rangle_\varepsilon$ being the retarded Green function thermally averaged over the eigenstates of the Hamiltonian (1).

Looking at equation (15), one sees that the LDOS depends on non-orthonormal fermionic operators:

$$\{\tilde{C}_{\varepsilon\sigma}^\dagger, c_{\varepsilon'\sigma}\} = \frac{\tilde{N}_\varepsilon}{\sqrt{\rho_0}}\delta(\varepsilon - \varepsilon')F_{\vec{R}}(\varepsilon), \tag{16}$$

where the spatial function $F_{\vec{R}}(\varepsilon)$ is given by

$$F_{\vec{R}}(\varepsilon) = \sum_{\vec{k}} \varphi_{\vec{k}}(\vec{R})\delta(\varepsilon - \varepsilon_k) = \rho_0 J_0(k(\varepsilon)R), \tag{17}$$

with J_0 being the zeroth-order Bessel function.

The operator (6) can be expressed in terms of fermionic operators orthonormal to $c_{\varepsilon\sigma}$ by introducing

$$\tilde{c}_{\varepsilon\sigma} = N_0\left(\tilde{C}_{\varepsilon\sigma} - \frac{\tilde{N}_0}{\sqrt{\rho_0}}F_{\vec{R}}(0)c_{\varepsilon\sigma}\right), \tag{18}$$

with a normalization factor evaluated at the Fermi level:

$$N_0 = \left\{1 - \left|\frac{\tilde{N}_0}{\sqrt{\rho_0}}F_{\vec{R}}(0)\right|^2\right\}^{-1/2}. \tag{19}$$

This leads to the following expression for $B_\sigma(\vec{R})$:

$$B_\sigma(\vec{R}) = \left[\frac{\int {\rm d}\varepsilon\, \tilde{c}_{\varepsilon\sigma}}{\tilde{N}_0 N_0} + \sqrt{2}\frac{F_{\vec{R}}(0)}{\rho_0} f_{0\sigma} + q_R^\sigma\sqrt{\pi\Gamma\rho_0}d_\sigma\right], \tag{20}$$

where we introduce an operator

$$f_{0\sigma} = \sqrt{\frac{\rho_0}{2}}\int c_{\varepsilon\sigma}\,{\rm d}\varepsilon, \tag{21}$$

which describes a conduction state centered at the adatom site.

As the Kondo effect occurs at low temperatures $T \ll T_{\rm K}$ and the tip bias is usually much smaller then the bandwidth, $eV \ll D$, we evaluate equation (12) at $T = 0$, thus resulting in

$$G(eV, T \ll T_{\rm K}, R) = \sum_\sigma G_{\rm max}^\sigma(\rho_{\rm tip}^\sigma/\rho_0)(\rho_{\rm LDOS}^\sigma/\rho_0) \tag{22}$$

where

$$G_{\rm max}^\sigma = (e^2/h)T_{o\sigma}\{1 + |q_R^\sigma|^2\} \tag{23}$$

and

$$\begin{aligned}\rho_{\rm LDOS}^\sigma/\rho_0 = {} & [1 - J_0^2(k_{\rm F}R)]\cos^2\delta_{q_R}^\sigma + \sin^2\delta_{q_R}^\sigma\sin^2\delta_{eV}^\sigma \\ & + 2J_0(k_{\rm F}R)\sin\delta_{q_R}^\sigma\cos\delta_{q_R}^\sigma\sin\delta_{eV}^\sigma\cos\delta_{eV}^\sigma \\ & + J_0^2(k_{\rm F}R)\cos^2\delta_{q_R}^\sigma\cos^2\delta_{eV}^\sigma.\end{aligned} \tag{24}$$

In the calculation of the above expression we used the Green function identities for the zero-temperature Anderson model [35]. The spin-dependent Fano factor phase shift $\delta_{q_R}^\sigma$ is defined as

$$\tan\delta_{q_R}^\sigma \equiv |q_R^\sigma|. \tag{25}$$

In equation (24) the terms proportional to $\sin^2\delta_{eV}^\sigma$ and $\cos^2\delta_{eV}^\sigma$ come from the direct tunneling paths tip–adatom–host and tip–host, respectively. The interference between them is given by the mixture term proportional to $\sin\delta_{eV}^\sigma\cos\delta_{eV}^\sigma$.

The spin-dependent phase shift $\delta_\varepsilon^\sigma$ for the conduction states can be determined from the Doniach–Sunjic spectral density [32, 33]:

$$\rho_{dd}^\sigma(eV) = \frac{1}{\pi\Gamma}{\rm Re}\left[\frac{{\rm i}\Gamma_{\rm K}}{(eV + \sigma\tilde{\Delta}) + {\rm i}\Gamma_{\rm K}}\right]^{\frac{1}{2}} = \frac{1}{\pi\Gamma}\sin^2\delta_{eV}^\sigma, \tag{26}$$

where $\tilde{\Delta}$ gives the Kondo peak splitting. According to [11, 14] the Kondo peak splitting comes from the ferromagnetic exchange interaction of the majority spin between the adatom and the STM tip. It gives rise to a local magnetic field at the adatom's site that leads to a Zeeman splitting $\tilde{\Delta}$ of the adatom's energy level:

$$\tilde{\Delta} = \varepsilon_{d\downarrow} - \varepsilon_{d\uparrow}, \tag{27}$$

which coincides with the Kondo peak splitting [11, 14].

The value of the splitting can be determined using a variety of methods, such as the self-consistent procedure [11, 15], scaling approach [11, 27], real-time diagrammatic technique [14] or numerical renormalization group simulations [10, 27]. Following [27], we put the Kondo peak splitting by hand in the adatom's spectral function (26) and for the sake of simplicity we adopt the 'poor man's' scaling approach [11, 27],[6] which estimates the splitting by

$$\begin{aligned}\tilde{\Delta} &= \frac{\Gamma_{\rm tip}^{\uparrow} + \Gamma_{\rm tip}^{\downarrow}}{2\pi} P_{\rm tip} \ln(D/U) \\ &= \left[\frac{\Gamma_{\rm tip}^{0}}{\pi} \ln(D/U)\right] P_{\rm tip} \exp(-2k_{\rm F}R),\end{aligned} \tag{28}$$

where $\Gamma_{\rm tip}^{0} = \pi |t_{dR=0}^{\sigma}|^2 \rho_0$ gives the local coupling between the Kondo adatom and an unpolarized tip. We use the expression

$$\Gamma_{\rm tip}^{\sigma} = \Gamma_{\rm tip}^{0}[1 + \sigma P_{\rm tip}] \exp(-2k_{\rm F}R), \tag{29}$$

to account for both spin and spatial dependences of the tip–adatom coupling.

4. Results

For numerical analysis we adopt the following set of model parameters: $\varepsilon_d^0 = -0.9$ eV, $\Gamma = 0.2$ eV, $U = 2.9$ eV, $D = 5.5$ eV, $T_{\rm K} = 50$ K and $k_{\rm F} = 0.189$ Å^{-1} [26, 27]. We consider the cases of large, small and intermediate Fano ratio values. For each of these cases we analyze the dependence of the conductance on tip–adatom lateral distance R. Additionally, for the large q limit we consider how the conductance depends on the asymmetry between tip–adatom and adatom–host couplings.

4.1. Large tip–adatom coupling ($q_{R=0} = 10$)

The large q limit has been achieved in experiments with an STM tip by employing magnetic molecules as Kondo adatoms [22, 23]. In this limit the host metal conduction electrons tunnel towards the tip, preferably via the localized magnetic adatom state. For the tip situated right above the adatom ($R = 0$), the conductance reveals an asymmetric splitting of the zero-bias anomaly (figure 2), characterized by a pair of peaks at $eV = -\tilde{\Delta}$ and $eV = \tilde{\Delta}$. Such asymmetry occurs due to the spin polarization of the tip (equation (11)), the higher peak corresponding to the majority spin-up states, while the lower one to the minority spin-down states.

[6] We note that in [27] the splitting $\tilde{\Delta}$ depends on $\Gamma_{\rm tip}^{\uparrow}$ and not on the sum of $\Gamma_{\rm tip}^{\uparrow} + \Gamma_{\rm tip}^{\downarrow}$ as was proposed in [11]. In our analysis we use the proposal of [11].

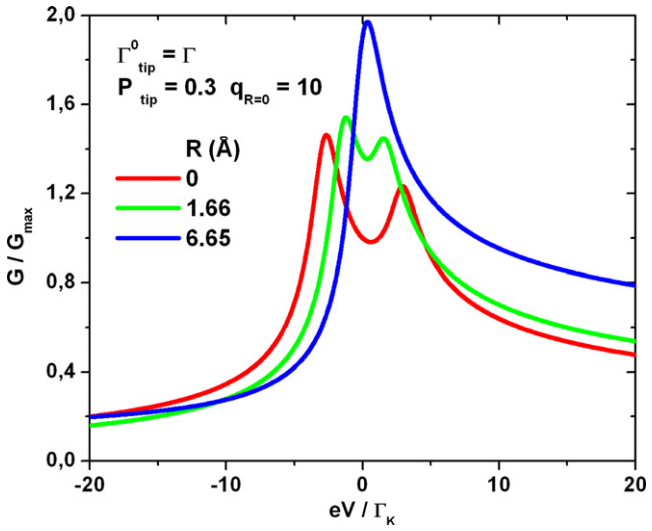

Figure 2. Conductance $G/G_{\rm max}$ as a function of the tip bias scaled in units of Kondo resonance half-width $eV/\Gamma_{\rm K}$ for $q_{R=0} = 10$ at three different tip lateral positions with symmetric potential barriers.

A similar asymmetric splitting of the Kondo peak was recently observed in a quantum dot system coupled to two ferromagnetic Ni electrodes [16, 17]. The large q limit in the system we consider resembles the standard case of a single dot in between leads without lead-to-lead direct coupling (embedded geometry). A wealth of theoretical works predict the spin splitting of the Kondo peak in a quantum dot system coupled to two ferromagnetic leads [10, 11, 15]. In those works this splitting was tuned via the relative angle between the left and the right lead magnetization [15], the lead's polarization [10] and an external magnetic field [11]. It was found for this last case that some adatoms with large spin ($S > 1/2$) deposited on a layer of Cu_2N have a Kondo peak splitting strongly dependent on the direction of an applied magnetic field [39]. The magnetic anisotropy of these adatoms in the presence of an inhomogeneous environment as the Cu_2N compound cause such behavior. As here we describe an adatom with spin $S = 1/2$ in a homogeneous host metal, magnetic anisotropy does not occur for the Kondo peak splitting.

Here we show one alternative/additional way to tune the spin splitting, by changing the tip–adatom separation (laterally or vertically)[7].

Increasing the tip–adatom lateral distance, the Fano ratio decays according to equation (10) and the Zeeman splitting of the Kondo peak quenches (see equation (28)). These effects can be seen at figure 2, where the conductance is plotted for three different values of the tip–adatom lateral distance. About $R = 6.65$ Å, the two resonances merge into a single peak, thus resulting in the standard Kondo resonance profile.

Not only the lateral tip–adatom separation can change the spin splitting, but also the vertical tip–adatom distance. To

[7] In the nonequilibrium regime, a system of a quantum dot coupled to a left and to a right normal electrode exhibits two Kondo resonances pinned at the Fermi levels of the leads [40]. The influence of ferromagnetic leads on this nonequilibrium Kondo effect was studied in [11].

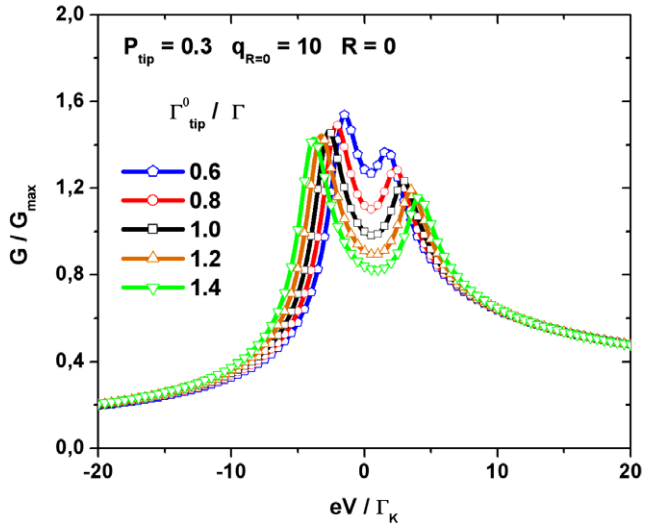

Figure 3. Conductance $G/G_{\max}$ at the origin as a function of the tip bias scaled in units of Kondo resonance half-width eV/Γ_K, for $q_{R=0} = 10$ and different potential barriers.

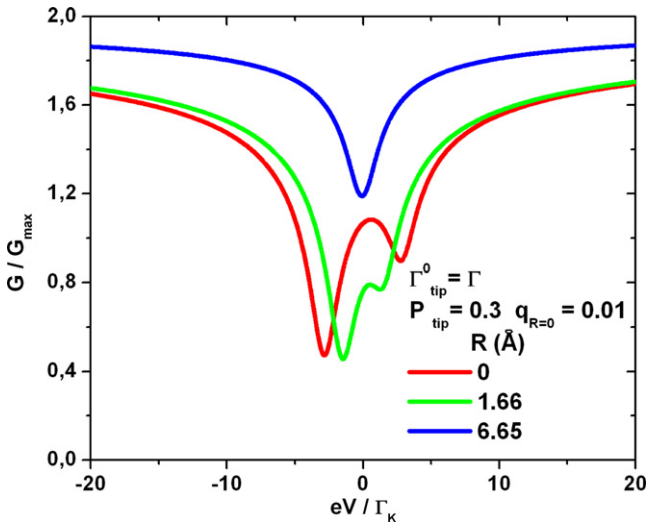

Figure 4. Conductance $G/G_{\max}$ as a function of the tip bias scaled in units of Kondo resonance half-width eV/Γ_K for $q_{R=0} = 0.01$ at three different tip lateral positions with symmetric potential barriers.

mimic this effect we change the ratio $\Gamma^0_{\rm tip}/\Gamma$, thus introducing an asymmetry between the tip–adatom ($\Gamma^0_{\rm tip}$) and adatom–host (Γ) tunneling rates.

For very short vertical tip–adatom distances, the proximity of the tip to the adatom shifts the adatom occupied level ε^0_d [41, 42] and, depending on the crystal surface orientation, changes the Kondo temperature [36]. For example, the Kondo temperature increases for Co on Cu(100) [41] while for Co on Cu (111) [42] it is kept constant. In particular for a ferromagnetic tip very close to the host metal surface, the RKKY (Ruderman–Kittel–Kasuya–Yosida) exchange interaction, intermediated by the host, would contribute to the conductance [27]. Since our simulations are for distances not very short, variations of the Kondo temperature and the RKKY interaction do not need to be included. Thus, moving the tip towards the adatom, the only effect expected in the present model is the increase of the coupling parameter $\Gamma^0_{\rm tip}$. Consequently, the splitting between the peaks becomes more apparent (see figure 3) which can be understood as a consequence of the enhancement of the local tip magnetic field on the adatom due to the tip proximity.

4.2. Small tip–adatom coupling ($q_{R=0} = 0.01$)

In the small coupling limit the conductance curves (figure 4) display dips instead of peaks observed in the large coupling limit (figures 2 and 3). The appearance of the dips at $eV = \pm\tilde{\Delta}$ is a consequence of a destructive quantum interference between the channels tip–host and tip–adatom–host. Thus it can be easily seen from equations (24) and (25) for $q \to 0$ and $R = 0$ that the LDOS behaves as

$$\rho^\sigma_{\rm LDOS}/\rho_0 = \cos^2 \delta^\sigma_{eV}, \tag{30}$$

which is opposite to the case $q_{R=0} \to \infty$, where

$$\rho^\sigma_{\rm LDOS}/\rho_0 = \sin^2 \delta^\sigma_{eV}. \tag{31}$$

As in the case of large coupling, the increase of the tip–adatom distance leads to a quenching of the anti-resonance splitting as can be seen comparing the curves corresponding to different values of R in figure 4. At $R = 6.65$ Å, the asymmetric zero-bias anomaly for the dips disappears and only the standard single anti-resonance profile is recovered. A single dip structure in the conductance for small q is verified for a system composed of Co on a Cu(111) surface [19, 21]. It is valid to note that, while the large q limit resembles the embedded geometry, the small q limit gives similar results to the T-shaped quantum dot (side-coupled geometry) [3, 43, 44].

4.3. Intermediate tip–adatom coupling ($q_{R=0} = 1$)

The intermediate case for a normal tip is characterized by the well-known Fano–Kondo lineshape [18, 21]. However, the introduction of a ferromagnetic tip results in distinct Fano–Kondo profiles for each spin component. The spin-up profile is shifted toward negative bias with an enhanced amplitude, while the spin-down case moves in the opposite direction, being reduced in amplitude. This is illustrated in the inset of figure 5, where we show $G^\uparrow/G_{\max}$ and $G^\downarrow/G_{\max}$.

The superposition of the spin-dependent Fano–Kondo profiles gives rise to the appearance of a plateau around the Fermi level ($eV = 0$) in the total conductance ($G^\uparrow + G^\downarrow$) for $R = 0$ (see figure 5). For large R ($R = 6.65$ Å), this plateau vanishes due to the suppression of the adatom's Zeeman splitting and standard Fano–Kondo results for the conductance with nonmagnetic tips are recovered [18, 21].

5. Conclusions

We derived a spin-resolved tunneling conductance for a system of a spin-polarized STM tip with a single Kondo adatom on the surface of a normal metallic host. The conductance dependence on the tip bias was investigated for different

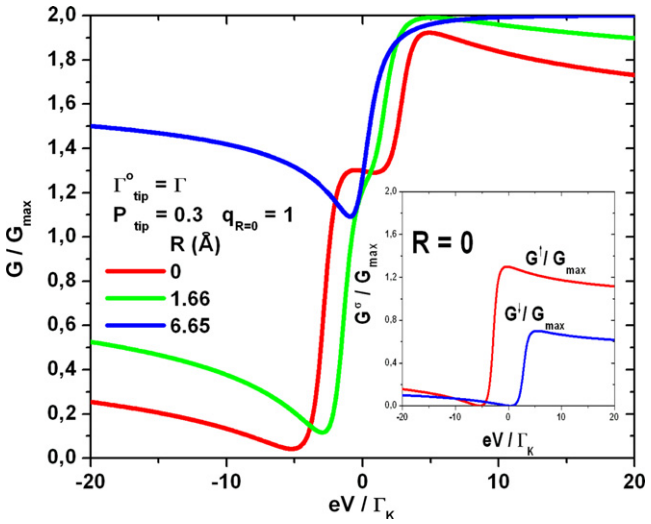

Figure 5. Conductance $G/G_{\max}$ as a function of the tip bias scaled in units of Kondo resonance half-width $eV/\Gamma_{\rm K}$ for $q_{R=0} = 1$ and three different tip lateral positions with symmetric potential barriers.

tip–adatom lateral distances for a wide range of the Fano parameter q, relevant for various experimental configurations. We demonstrated that the Fano parameter drastically affects the conductance pattern of the system. For large values of q, we observe an asymmetric splitting of the Kondo resonance which is suppressed with an increase of the tip–adatom lateral distance. For small q, the behavior of the conductance is opposite to those observed in the large q regime—instead of a split Kondo peak, one observes an asymmetrically split Kondo dip. For the intermediate case we have shown that, due to the splitting of the spin-resolved conductances ($G^{\uparrow} \neq G^{\downarrow}$), the total conductance exhibits a plateau in the region of small biases, which disappears for large enough values of a tip–adatom lateral distance.

Acknowledgments

We thank L N Oliveira and M Yoshida for stimulating discussions. This work was supported by the Brazilian agencies IBEM and CAPES.

Appendix

In this appendix we connect our main formulae (equations (24) and (26)) to the previously developed formalism [37, 38] and demonstrate how the Fano parameter (equation (9)) can be defined within the framework of our model (equation (3)). Adopting the notation $\vec{k} \equiv k$, we begin by considering the tunneling Hamiltonian (5) represented by

$$H_{\rm tun} = \sum_{p\sigma}\left[t_{\rm c}^{\sigma}\sum_{k}\varphi_k(\vec{R})a_{p\sigma}^{\dagger}c_{k\sigma} + t_{dR}^{\sigma}a_{p\sigma}^{\dagger}d_{\sigma} + \text{H.c.}\right], \tag{A.1}$$

where t_{dR}^{σ} and $t_{\rm c}^{\sigma}$ are the tip–adatom and tip–host hopping elements, respectively, $\varphi_k(\vec{R})$ is a conduction electron wavefunction evaluated at a surface position $\vec{R}$ laterally displaced from the adatom. Note that, in the Hamiltonian (A.1), the Fano factor (9) does not appear explicitly as in (6). Thus we calculate the spin-polarized conductance according to linear response theory [37, 38]. It leads to

$$\begin{aligned} G^{\sigma}(eV) = (2\pi)^2\left(\frac{e^2}{h}\right)\rho_{\rm tip}^{\sigma}\int {\rm d}\varepsilon\left[-\frac{\partial}{\partial\varepsilon}f(\varepsilon - eV)\right] \\ \times\left(-\frac{1}{\pi}\right){\rm Im}\left\{(t_{\rm c}^{\sigma})^2\sum_{kq}\varphi_k^{*}(\vec{R})G_{kq\sigma}^{\rm Ret}(\varepsilon)\varphi_q(\vec{R})\right. \\ + (t_{\rm c}^{\sigma})(t_{dR}^{\sigma})\sum_{k}\varphi_k^{*}(\vec{R})G_{kd\sigma}^{\rm Ret}(\varepsilon) \\ \left. + \ (t_{dR}^{\sigma})(t_{\rm c}^{\sigma})\sum_{k}G_{dk\sigma}^{\rm Ret}(\varepsilon)\varphi_k(\vec{R}) + (t_{dR}^{\sigma})^2G_{dd\sigma}^{\rm Ret}(\varepsilon)\right\}, \end{aligned} \tag{A.2}$$

with

$$G_{kq\sigma}^{\rm Ret}(\varepsilon) = \frac{\delta_{kq}}{\varepsilon - \varepsilon_k + {\rm i}\eta} + \frac{\sqrt{\frac{\Gamma}{\pi\rho_0}}}{\varepsilon - \varepsilon_k + {\rm i}\eta}G_{dq\sigma}^{\rm Ret}(\varepsilon) \tag{A.3}$$

and

$$G_{kd\sigma}^{\rm Ret}(\varepsilon) = \frac{\sqrt{\frac{\Gamma}{\pi\rho_0}}}{\varepsilon - \varepsilon_k + {\rm i}\eta}G_{dd\sigma}^{\rm Ret}(\varepsilon) \tag{A.4}$$

as the Fourier transforms of the time retarded Green's functions:

$$G_{kq\sigma}^{\rm Ret}(t-\tau) = -\frac{\rm i}{\hbar}\theta(t-\tau)\langle\{c_{k\sigma}(t), c_{q\sigma}^{\dagger}(\tau)\}\rangle, \tag{A.5}$$

$$G_{kd\sigma}^{\rm Ret}(t-\tau) = -\frac{\rm i}{\hbar}\theta(t-\tau)\langle\{c_{k\sigma}(t), d_{\sigma}^{\dagger}(\tau)\}\rangle \tag{A.6}$$

and

$$G_{dd\sigma}^{\rm Ret}(t-\tau) = -\frac{\rm i}{\hbar}\theta(t-\tau)\langle\{d_{\sigma}(t), d_{\sigma}^{\dagger}(\tau)\}\rangle, \tag{A.7}$$

respectively [1]. The energy representation of the adatom's Green function is

$$G_{dd\sigma}^{\rm Ret}(\varepsilon) = \frac{1}{\varepsilon - \varepsilon_{d\sigma} + {\rm i}\Gamma - \sum(\varepsilon)}, \tag{A.8}$$

where $\sum(\varepsilon)$ is the real part of the interacting self-energy [1].

The conductance for the Kondo regime is derived substituting equations (A.3) and (A.4) in (A.2) considering that

$$\left[-\frac{\partial}{\partial\varepsilon}f(\varepsilon - eV)\right] \sim \delta(\varepsilon - eV), \tag{A.9}$$

$$\sum_{k}\frac{1}{\varepsilon - \varepsilon_k + {\rm i}\eta} \sim -{\rm i}\pi\rho_0, \tag{A.10}$$

and

$$\sum_{k}\varphi_k(\vec{R}) \sim J_0(k_{\rm F}R)(2D\rho_0) \tag{A.11}$$

are valid approximations in the limit of $T \ll T_{\rm K}$ and $\varepsilon \ll D$. Thus we obtain the result

$$\begin{aligned} G^{\sigma}(eV) = (2\pi)^2\left(\frac{e^2}{h}\right)\rho_{\rm tip}^{\sigma}\rho_0(t_{\rm c}^{\sigma})^2 \\ \times\{[(q_R^{\sigma})^2 - J_0^2(k_{\rm F}R)]\pi\Gamma\rho_{dd}^{\sigma}(eV) \\ + 2\Gamma J_0(k_{\rm F}R)q_R^{\sigma}\,{\rm Re}\{G_{dd\sigma}^{\rm Ret}(eV)\} + 1\} \end{aligned} \tag{A.12}$$

in terms of the adatom's spectral density:

$$\rho_{dd}^{\sigma}(eV) = \left(-\frac{1}{\pi}\right) \mathrm{Im}\{G_{dd\sigma}^{\mathrm{Ret}}(eV)\} \tag{A.13}$$

and a parameter that we define according to equation (9). At this stage of the calculations as in [37, 38], this factor is recognized as the same asymmetry parameter of Fano's theory [28].

In particular, the standard Fano formula [28] for the conductance can only be obtained assuming a Lorentzian lineshape for the adatom's spectral density. For the Doniach–Sunjic description (equation (26)), equation (24) is derived instead. To that end, equation (23) and

$$\rho_{\mathrm{LDOS}}^{\sigma}(eV) = \rho^{\sigma}\{1 - [J_0^2(k_{\mathrm{F}}R) - (q_R^{\sigma})^2]\pi\Gamma\rho_{dd}^{\sigma}(eV) + 2\Gamma J_0(k_{\mathrm{F}}R) q_R^{\sigma}\,\mathrm{Re}\{G_{dd\sigma}^{\mathrm{Ret}}(eV)\}\} \tag{A.14}$$

with

$$\rho^{\sigma} = \frac{\rho_0}{1 + |q_R^{\sigma}|^2}, \tag{A.15}$$

as a normalization factor must be considered. The combination of them with the phases

$$\tan\delta_{eV}^{\sigma} = -\frac{\mathrm{Im}\{G_{dd\sigma}^{\mathrm{Ret}}(eV)\}}{\mathrm{Re}\{G_{dd\sigma}^{\mathrm{Ret}}(eV)\}} \tag{A.16}$$

and $\delta_{q_R}^{\sigma}$ (equation (25)) in (A.8) and (A.14) allow us to derive equation (24). The result (24), dependent on the factor q_R^{σ} (equation (9)), leads to the quantum interference effects predicted by Fano's theory [28] and are confirmed by the simulations of section 4.

References

[1] Hewson A C 1993 *The Kondo Problem to Heavy Fermions* (Cambridge: Cambridge University Press)
[2] Goldhaber-Gordon D, Shtrikman H, Mahalu D, Abusch-Magder D, Meirav U and Kastner M A 1998 *Nature* **391** 156
[3] Sato M, Aikawa H, Sano A, Katsumoto S and Yie Y 2005 *Phys. Rev. Lett.* **95** 066801
[4] Busser C A, Moreo A and Dagotto E 2004 *Phys. Rev.* B **70** 035402
[5] Lobos A M and Aligia A A 2006 *Phys. Rev.* B **74** 165417
[6] Sfigakis F, Ford C J, Pepper M, Kataoka M, Ritchie D A and Simmons M Y 2008 *Phys. Rev. Lett.* **100** 026807
[7] Tripathi V and Cooper N R 2008 *J. Phys.: Condens. Matter* **20** 164215
[8] For a review on spintronics see Zutic I, Fabian J and Das Sarma S 2004 *Rev. Mod. Phys.* **76** 323
[9] Zhang P, Xue Q K, Wang Y and Xie X C 2002 *Phys. Rev. Lett.* **89** 286803
[10] Martinek J, Sindel M, Borda L, Barnaś J, König J, Schön G and von Delft J 2003 *Phys. Rev. Lett.* **91** 247202
[11] Martinek J, Utsumi Y, Imamura H, Barnaś J, Maekawa S, König J and Schön G 2003 *Phys. Rev. Lett.* **91** 127203
[12] Mahn-Soo Choi, Sánchez D and López R 2004 *Phys. Rev. Lett.* **92** 056601
[13] Martinek J, Sindel M, Borda L, Barnaś J, Bulla R, König J, Schön G, Maekawa S and von Delft J 2005 *Phys. Rev.* B **72** 121302(R)
[14] Utsumi Y, Martinek J, Schön G, Imamura H and Maekawa S 2005 *Phys. Rev.* B **71** 245116
[15] Świrkowicz R, Wilczyński M, Wawrzyniak M and Barnaś J 2006 *Phys. Rev.* B **73** 193312
[16] Hamaya K, Kitabatake M, Shibata K, Jung M, Kawamura M, Hirakawa K, Machida T and Taniyama T 2007 *Appl. Phys. Lett.* **91** 232105
[17] Pasupathy A N, Bialczak R C, Martinek J, Grose J E, Donev L A K, McEuen P L and Ralph D C 2004 *Science* **306** 86
[18] Madhavan V, Chen W, Jamneala T, Crommie M F and Wingreen N S 1998 *Science* **280** 567
[19] Manoharan H C, Lutz C P and Eigler D M 2000 *Nature* **403** 512
[20] Madhavan V, Chen W, Jamneala T and Crommie F 2001 *Phys. Rev.* B **64** 165412
[21] Knorr N, Schneider M A, Diekhöner L, Wahl P and Kern K 2002 *Phys. Rev. Lett.* **88** 096804
[22] Wahl P, Diekhöner L, Wittich G, Vitali L, Schneider M A and Kern K 2005 *Phys. Rev. Lett.* **95** 166601
[23] Fu Y-S, Ji S-H, Chen X, Ma X-C, Wu R, Wang C-C, Duan W-H, Qiu X-H, Sun B, Zhang P, Jia J-F and Xue Q-K 2007 *Phys. Rev. Lett.* **99** 256601
[24] Aguiar-Hualde J M, Chiappe G, Louis E and Anda E V 2007 *Phys. Rev.* B **76** 155427
[25] Chiappe G and Louis E 2006 *Phys. Rev. Lett.* **97** 076806
[26] Újsághy O, Kroha J, Szunyogh L and Zawadowski A 2000 *Phys. Rev. Lett.* **85** 2557
[27] Patton K R, Kettemann S, Zhuravlev A and Lichtenstein A 2007 *Phys. Rev.* B **76** 100408(R)
[28] Fano U 1961 *Phys. Rev.* **124** 1866
[29] Shelykh I A and Galkin N G 2005 *Phys. Rev.* B **70** 05328
[30] Shelykh I A, Galkin N G and Bagraev N T 2006 *Phys. Rev.* B **74** 165331
[31] Moldoveanu V, Tolea M, Gudmundsson V and Manolescu A 2005 *Phys. Rev.* B **72** 085338
[32] Frota H O and Oliveira L N 1986 *Phys. Rev.* B **33** 7871
[33] Frota H O 1992 *Phys. Rev.* B **45** 1096
[34] Silver R N, Gubernatis J E, Sivia D S and Jarrell M 1990 *Phys. Rev. Lett.* **65** 496
[35] Anderson P W 1961 *Phys. Rev.* **124** 41
[36] Costi T A, Hewson A C and Zlatić V 1994 *J. Phys.: Condens. Matter* **6** 2519
[37] Schiller A and Hershfield S 2000 *Phys. Rev.* B **61** 9036
[38] Plihal M and Gadzuk J W 2001 *Phys. Rev.* B **63** 085404
[39] Otte A F, Ternes M, Bergmann K V, Loth S, Brune H, Lutz C P, Hirjibehedin and Heinrich A J 2008 *Nat. Phys.* **4** 847
[40] See Krawiec M and Wysokiński K I 2002 *Phys. Rev.* B **66** 165408
[41] Néel N, Kröger J, Limot L, Palotas K, Hofer W A and Berndt R 2007 *Phys. Rev. Lett.* **98** 016801
[42] Vitali L, Ohmann R, Stepanow S, Gambardella P, Tao K, Huang R, Stepanyuk V S, Bruno P and Kern K 2008 arXiv:cond-mat/0808.0585
[43] Seridonio A C, Yoshida M and Oliveira L N 2007 arXiv:cond-mat/0701529
[44] Lee W R, Kim J U and Sim H S 2008 *Phys. Rev.* B **77** 033305